

Resonance model study on $K^+N \rightarrow Kp\eta$ near threshold

Bo-Chao Liu*

Department of Applied Physics, Xi'an Jiaotong University, Xi'an, Shaanxi 710049, China

(Received 19 October 2011; revised manuscript received 15 June 2012; published 13 July 2012)

By using resonance model, we investigate $K^+N \rightarrow KN\eta$ reactions with the assumption that these reactions are dominated by the excitation of $N^*(1535)$ near threshold. It is found that the hyperon and ρ exchange diagrams give the most important contributions to these reactions. Thus, these reactions may be a good place to study the coupling of $N^*(1535)$ with $K\Lambda$, $K\Sigma$, and $N\rho$ channels. We demonstrate that the angular distributions of final particles provide useful information about the different mechanisms of the $N^*(1535)$ excitations, which could be useful for future experimental analysis on these reactions.

DOI: [10.1103/PhysRevC.86.015207](https://doi.org/10.1103/PhysRevC.86.015207)

PACS number(s): 13.75.-n, 14.20.Gk, 13.30.Eg

I. INTRODUCTION

The negative parity nucleon resonance $N^*(1535)$ is particularly interesting in light hadron physics because of its peculiar properties. It is the chiral partner ($J^P = \frac{1}{2}^-$) of the nucleon and has strong decay channels for both πN and ηN . Although it is ranked as a four-star state in Particle Data Group (PDG) [1], the nature and property of $N^*(1535)$ are still not well understood. Besides the conventional constituent quark model interpretation, it has also been argued that $N^*(1535)$ is a quasibound ($K\Sigma - K\Lambda$) state [2] and has large effective couplings to $K\Lambda$ and $K\Sigma$ [3]. To check these model predictions, experimental information on the coupling of $N^*(1535)$ with KY (kaon-hyperon) states should be necessary. Unfortunately, current experimental knowledge on these kaon-hyperon couplings is still poor, partly because of a lack of data on the experimental side and partly owing to the complication of various interfering t -channel exchange contributions [4] in πN and γN scatterings.

In recent years, the decay of J/Ψ is also utilized to study the properties of nucleon resonances [5]. Because the isospin of J/Ψ is zero, its decay offers a natural isospin filter which makes it a unique place to study the properties of nucleon resonances. In the reaction $J/\Psi \rightarrow pK^-\bar{\Lambda}$, it is found that there is an enhancement in $K\Lambda$ invariant mass spectrum near threshold [6]. If this enhancement is caused by $N^*(1535)$, it will imply that $N^*(1535)$ has a large coupling to $K\Lambda$ and will have important implications on the property and nature of $N^*(1535)$ [7,8]. Based on a similar picture, it is also argued that $N^*(1535)$ probably has large coupling to $N\phi$ [9–11]. Obviously, some further studies on the coupling of $N^*(1535)$ with KY states will be helpful to understand the nature of $N^*(1535)$ and relevant reaction mechanisms.

Besides the KY couplings, the coupling of $N^*(1535)$ with vector meson and nucleon is also not well determined, which causes the debate that whether π [12–14] or ρ [15–19] meson exchange diagram dominates η production in nucleon-nucleon collisions. The differences between these two kinds of models are generally related to the uncertainties of the coupling constant $g_{N^*(1535)N\rho}$. Even though the uncertainties of this

coupling constant are examined in detail in Ref. [20], it is still interesting and important to constrain the value of this coupling constant in some other channels.

With the problems mentioned above, it is natural to ask whether there are some other channels that are suitable for studying the properties of $N^*(1535)$. In this work, by using a resonance model we study the reactions $K^+p \rightarrow K^+p\eta$, $K^+n \rightarrow K^0p\eta$, and $K^+n \rightarrow K^+n\eta$ with the assumption that the excitation of $N^*(1535)$ dominates these reactions near threshold. Some other contributions to this channel are mainly from the excitation of the K^* resonances and other nucleon resonances besides $N^*(1535)$. Because we are only interested in the energy range near threshold, it is reasonable to expect that only the states which have S -wave coupling to $K\eta$ or $N\eta$ channel can give significant contributions. For the $K\eta$ channel, the K^* state in the relevant energy range that has S -wave coupling with $K\eta$ is $K_0^*(1430)$, which is about 400 MeV above the $K\eta$ threshold and should have minor effects near threshold. Furthermore, there is also some indirect evidence from the Dalitz plots [21,22] that show that K^* 's do not give significant contribution near threshold. For the subthreshold contribution from $K^*(892)$, we note that it has p -wave coupling to $K\eta$ and its mass is about 150 MeV below threshold. In view of its relatively small width, that is, 50 MeV, we expect that the contribution from $K^*(892)$ should also have minor effects near threshold. Meanwhile, according to PDG [1], we find that near the ηN threshold the S_{11} states $N^*(1535)$ and $N^*(1650)$ have significant decay branch ratios to both $N\rho$ and $N\eta$ channels and may give sizable contributions to these reactions. With the parameters and formulas offered in Ref. [23], we calculate the contribution from $N^*(1650)$ and find that its contribution is very small compared to the contribution from $N^*(1535)$ because of its larger mass and relatively weak coupling with the $N\eta$ channel. The dominance of $N^*(1535)$ in the $N\eta$ channel near threshold is also well identified in relevant experimental studies of $J/\Psi \rightarrow p\bar{p}\eta$ [24] and $pp \rightarrow pp\eta$ [25] reactions. Based on the considerations given above, we ignore the contribution from K^* 's and other nucleon resonances in present work. Owing to no clear evidence of the existence of pentaquark, we also ignore the s -channel pentaquark contributions.

In next section, we give the formalism and ingredients in our calculation, and then numerical results and some discussions

*liubc@xjtu.edu.cn

are given in Sec. III. A short summary is given in the last section.

II. THEORETICAL FORMALISM

In this work, we study the reactions $K^+p \rightarrow K^+p\eta$, $K^+n \rightarrow K^0p\eta$, and $K^+n \rightarrow K^+n\eta$ in an effective Lagrangian approach. We assume that these reactions are dominated by the intermediate excitation of the $N^*(1535)$ near threshold and then $N^*(1535)$ decays to $N\eta$. The basic Feynman diagrams for the $K^+N \rightarrow KN\eta$ are depicted in Fig. 1.

We use the commonly used interaction Lagrangians for ρKK , ωKK , and ϕKK couplings [26],

$$\mathcal{L}_{\rho K\bar{K}} = iG_V[\bar{K}\vec{\tau}(\partial_\mu K) - (\partial_\mu \bar{K})\vec{\tau}K] \cdot \vec{\rho}^\mu, \quad (1)$$

$$\mathcal{L}_{\omega K\bar{K}} = iG_V[\bar{K}(\partial_\mu K) - (\partial_\mu \bar{K})K]\omega^\mu, \quad (2)$$

$$\mathcal{L}_{\phi K\bar{K}} = -\sqrt{2}iG_V[\bar{K}(\partial_\mu K) - (\partial_\mu \bar{K})K]\phi^\mu. \quad (3)$$

At each vertex a relevant off-shell form factor is used. In our computation, we take the same form factors as that widely used [27]

$$F_V^{KK} = \frac{\Lambda_V^2 - m_V^2}{\Lambda_V^2 - q_V^2}, \quad (4)$$

where Λ_V , m_V , and q_V are the cutoff parameter, mass, and four-momentum for the exchanged meson (V) respectively. We adopt the coupling constant G_V and Λ_V as $G_V = 3.02$ and $\Lambda_V = 2$ GeV in the calculations [27].

To calculate the Feynman diagrams in Fig. 1, we still need to know the interaction Lagrangian involving $N^*(1535)$ resonance. In Ref. [28], a Lorentz covariant orbital-spin (L-S) scheme for N^*NM couplings has been given in detail. With this scheme, we can easily write the effective $N^*(1535)N\eta$,

$N^*(1535)N\rho$, $N^*(1535)N\omega$, and $N^*(1535)N\phi$ vertex functions,

$$V_{N^*(1535)N\eta} = ig_{N^*(1535)N\eta}\bar{u}_N u_{N^*(1535)} + \text{H.c.}, \quad (5)$$

$$V_{N^*(1535)N\rho} = ig_{N^*(1535)N\rho}\bar{u}_N \gamma_5 \left(\gamma_\mu - \frac{q_\mu \gamma^v q_v}{q^2} \right) \times \varepsilon^\mu(p_\rho) u_{N^*(1535)} + \text{H.c.}, \quad (6)$$

$$V_{N^*(1535)N\omega} = ig_{N^*(1535)N\omega}\bar{u}_N \gamma_5 \left(\gamma_\mu - \frac{q_\mu \gamma^v q_v}{q^2} \right) \times \varepsilon^\mu(p_\omega) u_{N^*(1535)} + \text{H.c.}, \quad (7)$$

$$V_{N^*(1535)N\phi} = ig_{N^*(1535)N\phi}\bar{u}_N \gamma_5 \left(\gamma_\mu - \frac{q_\mu \gamma^v q_v}{q^2} \right) \times \varepsilon^\mu(p_\phi) u_{N^*(1535)} + \text{H.c.} \quad (8)$$

Here u_N and u_{N^*} are the spin-wave functions for the nucleon and $N^*(1535)$ resonance; $\varepsilon^\mu(p_\rho)$, $\varepsilon^\mu(p_\omega)$, and $\varepsilon^\mu(p_\phi)$ are the polarization vectors of the ρ , ω , and ϕ mesons, respectively. It is worth noting that because the spin of vector meson is 1, both S -wave and D -wave L-S couplings are possible for the $N^*(1535)N\rho$, $N^*(1535)N\omega$, and $N^*(1535)N\phi$ interactions. It was found that the S -wave coupling has significant contribution to the $N^*(1535)$ decaying to $N\rho$ compared with the D wave [1,29]. In our calculations we consider only the S -wave $N^*(1535)$ resonance coupling to $N\rho$ and neglect the D -wave coupling. We also neglect the D -wave $N^*(1535)$ resonance couplings to $N\omega$ and $N\phi$ for simplicity as it was done in Ref. [9,10]. The monopole form factors for $N^*(1535)N$ -meson vertices are used,

$$F_{NM}^{N^*} = \frac{\Lambda^{*2} - m_V^2}{\Lambda^{*2} - q_V^2}, \quad (9)$$

where m_V and q_V are the mass and four-momentum of the exchanging vector mesons and we adopt $\Lambda^* = 1.3$ GeV [9] in our work. For the coupling constant $g_{N^*(1535)N\rho}$, we take $g_{N^*(1535)N\rho}^2/4\pi = 0.1$ [9] in our calculation which is determined by the partial decay width $\Gamma_{N^*(1535) \rightarrow N\rho \rightarrow N\pi\pi}$. It is shown in Ref. [20] that this value is also consistent with the prediction of the radiation decay of $N^*(1535)$ within vector meson dominance model. For the coupling constant $g_{N^*(1535)N\eta}$, we use the value $g_{N^*(1535)N\eta}^2/4\pi = 0.28$ [9], which is obtained from the partial decay width of $N^*(1535)$ to $N\eta$. The coupling constant $g_{N^*(1535)N\omega}$ is still not well constrained by experimental data. In the literature, the ratio of $g_{N^*(1535)N\rho}$ to $g_{N^*(1535)N\omega}$ varies from 1.77 to 2.6 [30–32]. In this work, we adopt the value of ratio as 2, which gives $g_{N^*(1535)N\omega}^2/4\pi = 0.25$. Another coupling constant $g_{N^*(1535)N\phi}$ is also not well known. However, in Ref. [9] it is shown that if assuming a large coupling of $N^*(1535)$ with $N\phi$, both $\pi^-p \rightarrow n\phi$ and $pp \rightarrow pp\phi$ data can be well described. So in this work, we adopt $g_{N^*(1535)N\phi}^2/4\pi = 0.13$, as suggested in Ref. [9]. Concrete calculations show that, even with this large coupling constant, ϕ exchange diagram only plays a minor role in these reactions.

The other class of Feynman diagram considered in this work is Fig. 1(b). The effective Lagrangians describing the couplings of $N^*(1535)$ to KY and N to KY are taken from

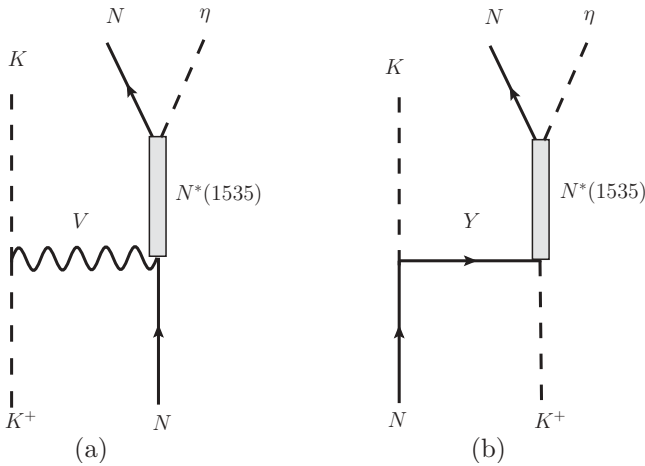


FIG. 1. Feynman diagrams for the excitation of $N^*(1535)$ through (a) vector meson exchange and (b) hyperon exchange in $K^+N \rightarrow KN\eta$ reactions. For $K^+p \rightarrow K^+p\eta$, $V = \rho^0$, ϕ , or ω and $Y = \Lambda$ or Σ^0 ; for $K^+n \rightarrow K^0p\eta$, $V = \rho^\pm$ and $Y = \Lambda$ or Σ^0 ; for $K^+n \rightarrow K^+n\eta$, $V = \rho^0$, ϕ , or ω and $Y = \Sigma^-$.

Ref. [7,8]:

$$\mathcal{L}_{N^*(1535)K\Lambda} = -ig_{N^*(1535)K\Lambda} \bar{\Psi}_{N^*(1535)} \Psi_{\Lambda} \Phi_K + \text{H.c.}, \quad (10)$$

$$\mathcal{L}_{N^*(1535)K\Sigma} = -ig_{N^*(1535)K\Sigma} \bar{\Psi}_{N^*(1535)} \vec{\tau} \cdot \vec{\Psi}_{\Sigma} \Phi_K + \text{H.c.}, \quad (11)$$

$$\mathcal{L}_{NK\Lambda} = ig_{NK\Lambda} \bar{\Psi}_N \gamma_5 \Psi_{\Lambda} \Phi_K + \text{H.c.}, \quad (12)$$

$$\mathcal{L}_{NK\Sigma} = ig_{NK\Sigma} \bar{\Psi}_N \gamma_5 \Psi_{\Sigma} \Phi_K + \text{H.c.} \quad (13)$$

For the value of coupling constants $g_{NK\Lambda}$ and $g_{NK\Sigma}$, one popular choice is to use SU(3) predictions. It has been shown that $pp \rightarrow pKY$ [33,34] and Kp scattering [35] can be understood in terms of $g_{K\Lambda p}$ and $g_{K\Sigma p}$ values which are in good agreement with the SU(3) predictions. Also from a Regge analysis of the high-energy $\gamma p \rightarrow KY$ data [36], it seems that the coupling constants are still in agreement with SU(3) predictions. So we adopt the SU(3) predicted values, that is, $g_{NK\Lambda}^2/4\pi = 14.06$ and $g_{NK\Sigma}^2/4\pi = 1.21$, in our calculations. For the coupling constants $g_{N^*K\Lambda}$ and $g_{N^*K\Sigma}$, one option is to determine them from SU(3) predictions, because it was shown in Ref. [37] that the SU(3) relations may hold for $N^*(1535)$. Within this option, one can follow the logic and results given in Ref. [38]. With the parameters given in that work, that is, $\alpha = -0.28$ and $|A_8| = 5.2$, we get $g_{N^*(1535)K\Lambda}^2/4\pi = 0.14$ and $g_{N^*(1535)K\Sigma}^2/4\pi = 5.24$ (Option I). The other option is to follow the results given in Ref. [3], where the ratio between $|g_{N^*(1535)K\Lambda}|$, $|g_{N^*(1535)K\Sigma}|$ and $|g_{N^*(1535)N\eta}|$ can be obtained as 0.92 : 1.5 : 1.84. With the value of $g_{N^*(1535)N\eta}$ given above, then we get $g_{N^*(1535)K\Lambda}^2/4\pi = 0.069$ and $g_{N^*(1535)K\Sigma}^2/4\pi = 0.19$ (Option II). By comparing these two options, we find that for the coupling constant $g_{N^*(1535)K\Lambda}$ these two options give some similar predictions, while, for the coupling constant $g_{N^*(1535)K\Sigma}$, the predictions from these two options are very different. The SU(3) prediction for $g_{N^*(1535)K\Sigma}$ is about 5.3 times larger than that obtained from Ref. [3]. With this uncertainty in mind, we adopt Option II in the following calculations, because with a very large $g_{N^*(1535)K\Sigma}$ it may cause problems in consistently describing some other relevant processes, such as $\gamma p \rightarrow K\Sigma$ or $\pi^- p \rightarrow K\Sigma$ reactions, where $N^*(1535)$ also contributes. The final conclusion on the value of $g_{N^*(1535)K\Sigma}$ should be made with a thorough analysis of all relevant channels. The form factors for the vertices NKY and N^*KY are taken from Ref. [39]:

$$F_{KY} = \frac{\Lambda_u^4}{\Lambda_u^4 + (q^2 - m^2)^2}. \quad (14)$$

For the cutoff parameter of vertex $KN\Lambda$, it is known that to control the Born amplitudes of reaction $\gamma p \rightarrow K^+\Lambda$ in a reasonable range the introduction of a mechanism that reduces the Born strength is necessary [39]. One possible way is to introduce a rather small Λ_u , and it is shown that the experimental data can be described fairly well with $\Lambda_u = 0.4$ GeV [40,41]. However, with such a small Λ_u , the form factors play a predominant role in the reaction dynamics and may cause serious questions about the validity of the theoretical framework. Also, using such a small value of

TABLE I. Coupling constants and cutoff parameters adopted in present work.

Vertex	g	Λ (GeV)	Vertex	$g^2/4\pi$	Λ (GeV)
ρKK	$G_V = 3.02$	2.0	$N^*(1535)N\rho$	0.1	1.3
ωKK	G_V	2.0	$N^*(1535)N\omega$	0.25	1.3
ϕKK	$\sqrt{2}G_V$	2.0	$N^*(1535)N\phi$	0.13	1.3
$NK\Lambda$	-13.29	1.5	$N^*(1535)K\Lambda$	0.069	1.3
$NK\Sigma$	3.9	1.5	$N^*(1535)K\Sigma$	0.19	1.3
			$N^*(1535)N\eta$	0.28	

Λ_u one cannot give consistent descriptions of the reaction $ep \rightarrow eK^+\Lambda$ as well [42]. So we adopt $\Lambda_u = 1.5$ GeV for vertex $KN\Lambda$ in our work as suggested in Ref. [39]. To reduce the number of free parameters, we use the same cutoff parameter for the vertex $KN\Sigma$ as well. For the vertices $N^*(1535)K\Lambda$ and $N^*(1535)K\Sigma$ in a u channel, we use the same form factor as that defined in Eq. (14). However, the cutoff parameter (Λ_u^*) for these vertices is not well determined in the literature. In this work, we adopt $\Lambda_u^* = 1.3$ GeV for these vertices, and the uncertainties owing to this parameter are discussed below. For easy comparison with other works, all the coupling constants and cutoff parameters adopted in our work are collected in Table I.

The $N^*(1535)$ propagator is written in a Breit-Wigner form [43]:

$$G_{N^*}(q) = \frac{i(q + M_{N^*})}{q^2 - M_{N^*}^2 + iM_{N^*}\Gamma_{N^*}(q^2)}, \quad (15)$$

where $\Gamma_{N^*}(q^2)$ is the energy-dependent total width and q is the four-momentum of $N^*(1535)$. Keeping only the dominant πN and ηN decay channels [1], this can be decomposed as

$$\Gamma_{N^*}(q^2) = a_{\pi N} \rho_{\pi N}(q^2) + b_{\eta N} \rho_{\eta N}(q^2), \quad (16)$$

where $a_{\pi N} = 0.12$ GeV/c², $b_{\eta N} = 0.32$ GeV/c², and the two-body phase space factors, $\rho_{\pi(\eta)N}(q^2)$, are

$$\rho(q^2) = 2p^{\text{cm}}(q^2) \Theta(q^2 - q_{\text{thr}}^2) \sqrt{q^2}, \quad (17)$$

and q_{thr} is the threshold value for the decay channel.

The propagators of vector meson and hyperon are also needed in the calculations and can be written in the form

$$G_V^{\mu\nu}(q_V) = -i \left(\frac{g^{\mu\nu} - q_V^\mu q_V^\nu / q_V^2}{q_V^2 - m_V^2} \right), \quad (18)$$

$$G_Y(q_Y) = i \frac{q_Y + M_Y}{q_Y^2 - m_Y^2}, \quad (19)$$

where q_V and q_Y are the four-momentum of the exchanged vector meson and hyperon ($Y = \Lambda$ or Σ), respectively.

After having established the effective Lagrangians, coupling constants, and form of the propagators, the invariant scattering amplitudes can be written by following the standard Feynman rules. The calculations of the differential and total

cross sections are then straightforward,

$$d\sigma = \frac{1}{16} \frac{m_N^2}{\sqrt{(p_K \cdot p_N)^2 - m_N^2 m_K^2}} \frac{1}{(2\pi)^5} \sum_{s_i, s_f} |\mathcal{M}_{fi}|^2 \times \prod_{a=1}^3 \frac{d^3 p_a}{E_a} \delta^4(P_i - P_f), \quad (20)$$

where \mathcal{M}_{fi} represents the total amplitude, P_i and P_f represent the sum of all the momenta in the initial and final states, respectively, and p_a denotes the momenta of the three particles in the final state.

III. RESULTS AND DISCUSSIONS

With the formalism and ingredients given above, the total cross sections versus excess energy Q for the $K^+p \rightarrow K^+p\eta$, $K^+n \rightarrow K^+n\eta$, and $K^+n \rightarrow K^0p\eta$ are calculated by using a Monte Carlo multiparticle phase space integration program. In Fig. 2, we show the results of cross sections obtained by considering vector meson exchange and hyperon exchange diagrams.

From Fig. 2, it can be found that the Λ , Σ , and ρ exchanges give the most important contributions to these reactions. The ϕ exchange contribution only plays a minor role, although we adopt a large value for $g_{N^*(1535)N\phi}$. The strength of ω exchange is a little smaller than ϕ exchange within our model.

In $K^+p \rightarrow K^+p\eta$, the Λ exchange dominates this reaction near threshold. The contribution from Σ exchange is much smaller than Λ exchange, which is mainly attributable to the large difference between the values of $g_{KN\Lambda}$ and $g_{KN\Sigma}$. While for the reaction $K^+n \rightarrow K^+n\eta$, Σ exchange plays the most important role. This is partly because Λ exchange is forbidden in this reaction and partly because Σ exchange is enhanced in this channel because of the isospin Clebsch-Gordan coefficients appearing in the vertex functions. In the reaction $K^+n \rightarrow K^0p\eta$, ω and ϕ exchanges are forbidden and ρ exchange becomes more important compared to other channels. The ρ exchange gives equally important contribution as Λ exchange. It is also because of the isospin Clebsch-Gordan coefficients appearing in the vertices that make ρ exchange much more favored in this reaction.

To check the dependence of the results on the cutoff parameter Λ_u^* adopted for $N^*(1535)KY$ vertex, we also perform the calculations with $\Lambda_u^* = 1.0$ GeV and $\Lambda_u^* = 2.0$ GeV, respectively. With a smaller cutoff value, that is, 1.0 GeV, the strength of the Λ and Σ exchange amplitudes is suppressed and their contributions to the cross section are reduced by a factor of 3. However, with $\Lambda_u^* = 2.0$ GeV, the contributions from Λ and Σ exchanges are enhanced by a factor of 2. The uncertainties owing to this parameter, which are obtained by varying the Λ_u^* from 1.0 to 2.0 GeV, are shown in Fig. 2 by the gray and shadowed area for Λ exchange and Σ exchange, respectively. The error bands show that the value of this cutoff parameter is important for determining the magnitudes

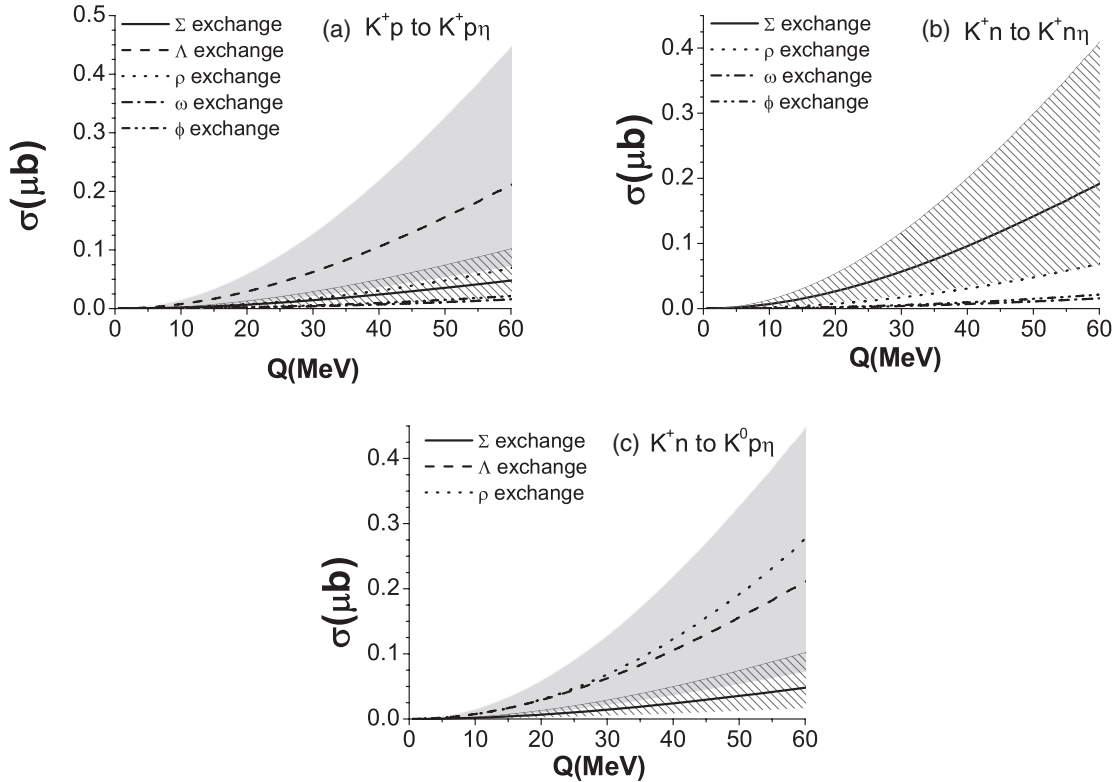


FIG. 2. The total cross section obtained by considering individual diagrams for reactions (a) $K^+p \rightarrow K^+p\eta$, (b) $K^+n \rightarrow K^+n\eta$, and (c) $K^+n \rightarrow K^0p\eta$, where the gray and shadowed areas denote the uncertainties owing to the cutoff parameters on $N^*(1535)K\Lambda$ and $N^*(1535)K\Sigma$, respectively.

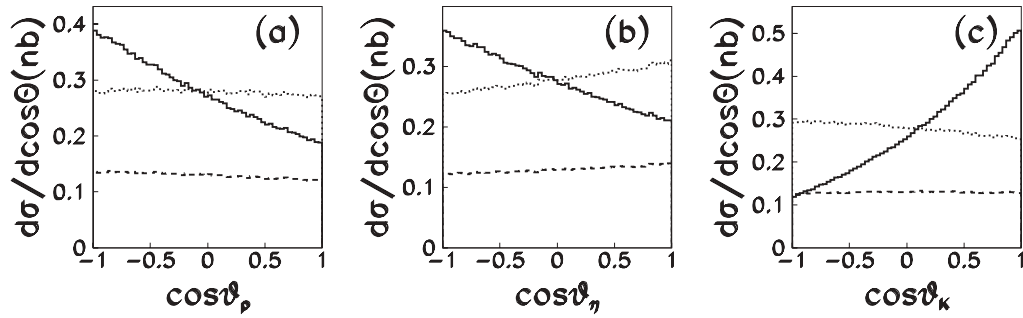


FIG. 3. Angular distribution of final proton (a), η (b), and K^0 (c) of the reaction $K^+n \rightarrow K^0 p \eta$, where θ denotes the angle of the outgoing particles relative to the incident K^+ beam direction in the c.m. frame. The solid, dashed, and dotted lines represent the contribution from ρ , Σ , and Λ exchange amplitudes, respectively.

of amplitudes. Unfortunately, because the cutoff parameter is introduced phenomenologically, it only can be determined by fitting to experimental data. Without experimental data near threshold, this parameter cannot be well determined in the present model. However, the above calculations may offer us some estimation about the uncertainties of the present model.

With the uncertainties mentioned above, it still can be expected from the results shown in Fig. 2 that the Λ , Σ , and ρ exchanges play the most important roles in the reactions $K^+N \rightarrow KN\eta$ near threshold. Thus, these reactions may constitute a good basis for investigating the couplings of $N^*(1535)$ with KY and $N\rho$ channels. Owing to the charge conservation law, Λ exchange is forbidden in $K^+n \rightarrow K^+n\eta$. Because Σ exchange dominates this reaction, this reaction may be a good place to extract the coupling constant $g_{N^*(1535)K\Sigma}$. Similarly, because Λ and ρ exchanges give the most important contributions to the reactions $K^+p \rightarrow K^+p\eta$ and $K^+n \rightarrow K^0p\eta$, these reactions are suitable to study the coupling constants $g_{N^*(1535)K\Lambda}$ and $g_{N^*(1535)N\rho}$.

To distinguish the contributions between hyperon and ρ exchanges, one possible way is to utilize the angular distribution of final particles in the c.m. frame. To illustrate this possibility, we show the angular distribution of final particles in the reaction $K^+n \rightarrow K^0p\eta$ in c.m. system at $Q = 15$ MeV in Fig. 3 by considering Λ , Σ , and ρ exchanges, respectively, where ρ and Λ exchanges have similar strength and Σ exchange only plays a minor role. Note that here we choose

the energy $Q = 15$ MeV just as an example, and the angular distributions do not change significantly near threshold. As can be seen from Fig. 3, the angular distribution from ρ exchange amplitude and hyperon exchange amplitude are distinct from each other. The pattern of angular distributions shown in Fig. 3 can be understood in the following way. If we ignore the decay of $N^*(1535)$, the ρ and hyperon exchange diagrams are corresponding to t -channel and u -channel diagrams, respectively. So one may expect that the angular distribution of the final K meson should have a forward peak for the ρ exchange amplitude and have a backward peak for the hyperon exchange amplitude. This is what we get in Fig. 3.

To investigate the interference effects, we need to fix the relative phase among individual amplitudes which, in principle, should be done by fitting to the data within an effective Lagrangian approach. To get an estimation of the interference effects, in this work we assume that the relative phase between Λ exchange amplitude and Σ exchange amplitude is fixed by the SU(3) symmetry; that is, we adopt the SU(3) predicted sign for the relevant coupling constants. The relative phase between ρ exchange amplitude and Λ exchange amplitude is taken to be either $+1$ or -1 , corresponding to the constructive and destructive interference, respectively. In this way, we can fix the relative phases among individual amplitudes and the corresponding results for the angular distributions are shown in Fig. 4, where we present the results by considering the coherent sum of the ρ and Λ exchanges [Fig. 4(a)], ρ and Σ exchanges

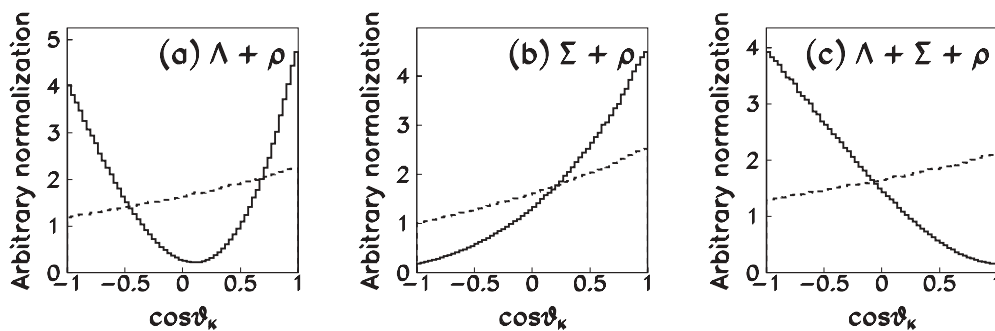


FIG. 4. Illustration of the interference effects on the angular distribution of final K meson in the c.m. frame in the $K^+n \rightarrow K^0p\eta$ reaction by considering the interference among ρ , Σ , and Λ exchange amplitudes. The solid and dashed lines represent the results corresponding to destructive and constructive interference, respectively. θ is defined in the same way as in Fig. 3.

[Fig. 4(b)], and the full mechanisms [Fig. 4(c)], respectively. It needs to be noted that significant interference effects among individual amplitudes are also found in the calculation of total cross sections. However, to show the interference effects on the shape of the angular distribution more clearly, we normalize individual results to the same quantity. As can be seen from Fig. 4, the interference between individual mechanisms may alter the angular distribution considerably compared to the distribution from the individual mechanisms without interference effects in Fig. 3. This shows clearly that the interference effects may have important influence on the physical observables.

Based on the above discussions, it can be expected that the experimental data of angular distributions may present very different pattern as compared to the angular distributions shown in Fig. 3 where interference effects are not taken into account. This will make it difficult to extract the relevant couplings from the experimental data directly. Here we want to note that the strength and relative roles of Σ and ρ exchanges change in different reactions. This means that if the angular distributions are sensitive to the relative phase and magnitude of individual amplitudes as shown in Fig. 4, the angular distributions of final particles would vary significantly in different reactions. Because the three reactions considered in this work are related by isospin symmetry, the strength of individual mechanism in different reactions is related by isospin relations. Thus, a combined analysis of all these three reactions can put strong constraints on the magnitude and relative phase of individual amplitudes, which will help us understand the coupling of $N^*(1535)$ with various channels

better. The specific features of angular distributions owing to individual mechanisms given in present work could be helpful for analyzing the reaction mechanisms when experimental data are available.

IV. SUMMARY

In this work, we study the reactions $K^+N \rightarrow KN\eta$ near threshold within an effective Lagrangian approach. Based on the assumption that this reaction is dominated by the excitation of $N^*(1535)$ resonance, we find that the Λ , Σ , and ρ exchange diagrams give the most important contributions to these reactions near threshold. Thus, the reactions under study may constitute a good basis to study the coupling of $N^*(1535)$ with $N\rho$, $K\Lambda$, and $K\Sigma$ channels. It is also found that interference effects among individual mechanisms are important and may alter the angular distributions significantly. A combined analysis on all the three reactions can help us better understand the relative roles of individual mechanisms, and the results of this work should be useful for analyzing and entangling the different mechanisms when the experimental data are available in the future.

ACKNOWLEDGMENTS

We acknowledge Zhen Ouyang and Ju-Jun Xie for their careful reading the manuscript and useful suggestions. This work is supported by the National Natural Science Foundation of China under Grant No. 10905046.

-
- [1] K. Nakamura *et al.*, *J. Phys. G* **37**, 075021 (2010).
 [2] N. Kaiser, P. B. Siegel, and W. Weise, *Phys. Lett. B* **362**, 23 (1995); N. Kaiser, T. Waas, and W. Weise, *Nucl. Phys. A* **612**, 297 (1997).
 [3] T. Inoue, E. Oset, and M. J. Vicente Vacas, *Phys. Rev. C* **65**, 035204 (2002).
 [4] G. Penner and U. Mosel, *Phys. Rev. C* **66**, 055211 (2002).
 [5] BES Collaboration, *Phys. Lett. B* **510**, 75 (2001); H. B. Li *et al.* (BES), *Nucl. Phys. A* **675**, 189c (2000).
 [6] H. X. Yang *et al.* (BES Collaboration), *Int. J. Mod. Phys. A* **20**, 1985 (2005).
 [7] B. C. Liu and B. S. Zou, *Phys. Rev. Lett.* **96**, 042002 (2006).
 [8] B. C. Liu and B. S. Zou, *Phys. Rev. Lett.* **98**, 039102 (2007).
 [9] J. J. Xie, B. S. Zou, and H. C. Chiang, *Phys. Rev. C* **77**, 015206 (2008).
 [10] J. Shi, J. P. Dai, and B. S. Zou, *Phys. Rev. D* **84**, 017502 (2011).
 [11] X. Cao, J. J. Xie, B. S. Zou, and H. S. Xu, *Phys. Rev. C* **80**, 025203 (2009).
 [12] M. Batinić, A. Svarc, and T.-S. H. Lee, *Phys. Scr.* **56**, 321 (1997).
 [13] K. Nakayama, in Proceedings of Symposium on Threshold Meson Production in p p and p d Interaction (COSY-11), Cracow, Poland, 2001, [arXiv:nuc1-th/0108032](https://arxiv.org/abs/nuc1-th/0108032).
 [14] R. Shyam, *Phys. Rev. C* **75**, 055201 (2007).
 [15] A. Moalem, E. Gedalin, L. Rzdolskaya, and Z. Shorer, *Nucl. Phys. A* **600**, 445 (1996); E. Gedalin, A. Moalem, and L. Rzdolskaya, *ibid.* **634**, 368 (1998).
 [16] A. B. Santra and B. K. Jain, *Nucl. Phys. A* **634**, 309 (1998).
 [17] G. Fäldt and C. Wilkin, *Phys. Scr.* **64**, 427 (2001).
 [18] K. Nakayama, J. Speth, and T.-S. H. Lee, *Phys. Rev. C* **65**, 045210 (2002).
 [19] T. Vetter, A. Engel, T. Biró, and U. Mosel, *Phys. Lett. B* **263**, 153 (1991).
 [20] J. J. Xie, C. Wilkin, and B. S. Zou, *Phys. Rev. C* **77**, 058202 (2008).
 [21] P. Rubin *et al.*, *Phys. Rev. Lett.* **93**, 111801 (2004).
 [22] V. Nomokonov *et al.*, *Nucl. Phys. A* **655**, 243c (1999).
 [23] X. Cao, B. S. Zou, and H. S. Xu, *Phys. Rev. C* **81**, 065201 (2010).
 [24] J. Z. Bai *et al.*, *Phys. Lett. B* **510**, 75 (2001).
 [25] R. Czyzykiewicz *et al.*, *Phys. Rev. Lett.* **98**, 122003 (2007).
 [26] D. V. Bugg, A. V. Sarantsev, and B. S. Zou, *Nucl. Phys. B* **471**, 59 (1996); L. Li, B. S. Zou, and G. L. Li, *Phys. Rev. D* **63**, 074003 (2001); **67**, 034025 (2003).
 [27] F. Q. Wu, B. S. Zou, L. Li, and D. V. Bugg, *Nucl. Phys. A* **735**, 111 (2004).
 [28] B. S. Zou and F. Hussain, *Phys. Rev. C* **67**, 015204 (2003).
 [29] T. P. Vrana, S. A. Dytman, and T.-S. H. Lee, *Phys. Rep.* **328**, 181 (2000).
 [30] A. B. Santra and B. K. Jain, *Nucl. Phys. A* **634**, 309 (1998).
 [31] T. Vetter, A. Engel, T. Biro, and U. Mosel, *Phys. Lett. B* **263**, 153 (1991).

- [32] E. Gedalin, A. Moalem, and L. Razdolskaja, *Nucl. Phys. A* **634**, 368 (1998).
- [33] A. Gasparian, J. Haidenbauer, C. Hanhart, L. Kondratyuk, and J. Speth, *Nucl. Phys. A* **684**, 397c (2001).
- [34] B. Holzenkamp, K. Holinde, and J. Speth, *Nucl. Phys. A* **500**, 485 (1989).
- [35] A. D. Martin, *Nucl. Phys. B* **179**, 33 (1981).
- [36] M. Guidal, J.-M. Laget, and M. Vanderhaeghen, *Nucl. Phys. A* **627**, 645 (1997).
- [37] A. Starostin, B. M. K. Nefkens *et al.*, *Phys. Rev. C* **64**, 055205 (2001).
- [38] N. P. Samios, M. Goldberg, and B. T. Meadows, *Rev. Mod. Phys.* **46**, 49 (1974).
- [39] S. Janssen, Jan Ryckebusch, D. Debruyne, and T. Van Cauteren, *Phys. Rev. C* **65**, 015201 (2001).
- [40] S. Janssen, J. Ryckebusch, W. Van Nespen, D. Debruyne, and T. Van Cauteren, *Eur. Phys. J. A* **11**, 181 (2001).
- [41] T. Mart and C. Bennhold, *Phys. Rev. C* **61**, 012201(R) (1999).
- [42] S. Janssen, J. Ryckebusch, and T. Van Cauteren, *Phys. Rev. C* **67**, 052201(R) (2003).
- [43] W. H. Liang *et al.*, *J. Phys. G* **28**, 333 (2002).